Third KSME-JSME
Thermal Engineering Conference
October 20-23, 1996
Kyongju, Korea

LIMITING THROTTLING LOSSES BY INTRACYCLE EVAPORATIVE COOLING

Byung Soon Kim, LG Electronics, Changwon City, 641-315 Korea

Piotr A. Domanski, NIST, Gaithersburg, MD 20899, USA

ABSTRACT

The temperature glide of zeotropic mixtures during phase change provides the opportunity to limit throttling losses of the refrigeration cycle by intracycle evaporative cooling of the refrigerant leaving the condenser. The difference between the intracycle evaporative cooling and the liquid-line/suction-line heat exchanger, instead of superheated vapor, is that a two-phase low-pressure refrigerant is used to subcool the high-pressure liquid leaving the condenser. The merits of the intracycle evaporative cooling were evaluated by a semi-theoretical simulation model and in the NIST's Small Breadboard Heat Pump at the cooling mode operating condition typical for a water-to-water residential heat pump. The capacity, coefficient of performance (COP), pressures, and temperature profiles of refrigerant and heat-transfer fluid in the heat exchangers are reported. The laboratory measured improvement of the COP was 4.0% for R32/152a(50/50), 3.6% for R407C, and 1.8% for R23/152a(20/80).

INTRODUCTION

Throttling losses during adiabatic expansion have a dual negative effect on the Coefficient of Performance (COP) of the vapor-compression cycle. These losses reduce system capacity and result in increased cycle work due to the lost expansion work of the throttled refrigerant. Different modifications to the vapor compression cycle[1] (economizer, liquid-line/suction-line heat exchanger (llsl-hx), two - phase turbine, ejector) can be used to limit the expansion losses of single-component refrigerants and mixtures. Besides these methods, intracycle evaporative cooling (IEC) of the refrigerant leaving the condenser by the low-pressure evaporating refrigerant provides an additional opportunity for reducing throttling losses of zeotropic mixtures. This method can only be applied to zeotropes due to their temperature glide during phase change. The COP can be improved when heat transfer between the low-pressure and high-pressure refrigerant results in an increased evaporator pressure and smaller specific compression work. Intracycle evaporative cooling was originally discussed by Vakil[2].

Different quality ranges of the two-phase, low-pressure refrigerant can be used for intracycle cooling. Mulroy et al.[3] studied the effect of intracycle cooling in a system with a three-passage evaporator. They directed the high-pressure refrigerant through one of these passages, counter-flow to the evaporating low-pressure refrigerant. The third passage was used by the heat-transfer fluid(HTF). Depending on mixture composition, the experimental data for R13/12 showed 5-10% COP improvement. In the same apparatus, little effect due to intracycle heat exchange was observed for R22/114.

Inctracycle evaporative cooling can aslo be accomplished with an intracycle heat exchanger(ic-hx) that is typically used for heat transfer between the liquid line and suction line, as shown in Figure 1. In this system, the high-pressure refrigerant leaving the condenser is subcooled by a low-pressure refrigerant leaving the evaporator (instead of superheat vapor, as it is done in the llsl-hx system). Figure 2 presents a thermodynamic diagram for the basic refrigeration cycle and the modified, IEC cycle. For the modified cycle, the figure shows the cycle realized for the limiting case of maximum heat transfer. This heat-transfer limit is indicated by the liquid (point 3') reaching the lowest temperature of the two-phase refrigerant in the evaporator (point 4'). It should be realized that the total benefit of intracycle heat exchange may have two sources: (1) an increased subcooling at the expansion device inlet and the systems response by increasing evaporator pressure and (2) a better use of the evaporator's heat-transfer area with two-phase refrigerant at the evaporator exit(no superheat). Figure 2 is simplified because it does not show an increased evaporator pressure as a result of intracycle heat transfer.

The study considered four refrigerants:R22, R407C(R32/125/134a(23/25/52)), R32/152a (50/50), and R23/152a(20/80), with R22 being selected as a reference. These refrigerants were selected to support a water-to-water residential heat pump[4,5] project involving these fluids.

Table 1 contains selected properties of the refrigerants studied. Except R22, the selected fluids have zero ozone depletion potential (ODP). R407C and R32/152a have comparable linear glides, while R23/152a has a larger and more nonlinear glide, as shown in Figure 3. Among the fluids tested, the R32/152a mixture has superior transport properties. All refrigerant properties in this study were calculated using subroutines from REFPROP.[6] These subroutines employed the Carnahan-Starling-DeSantis equation of state for calculating thermodynamic properties.

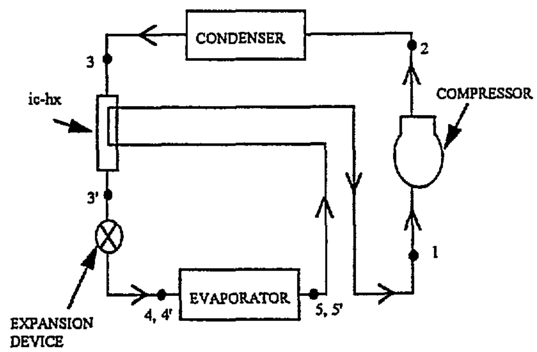

Figure 1. Schematic of a system implementing intracycle evaporative cooling

SIMULATIONS

The ic-hx cycle in Figure 2 was simulated using CYCLE-11, NIST's semitheoretical model.[4,7] CYCLE-11 performs simulations at imposed temperatures of the heat-transfer fluids (HTFs), which are specified at the inlet and outlet of the evaporator and condenser. In the version of CYCLE-11 used in this study, these heat exchangers were represented by their overall conductances (UA), which also are specified as input. It is assumed in the model that the heat-transfer conductance is constant throughout the heat exchanger regardless of refrigerant phase or quality. For the purpose of this study, the model was modified to enable simulating the cycle of interest.

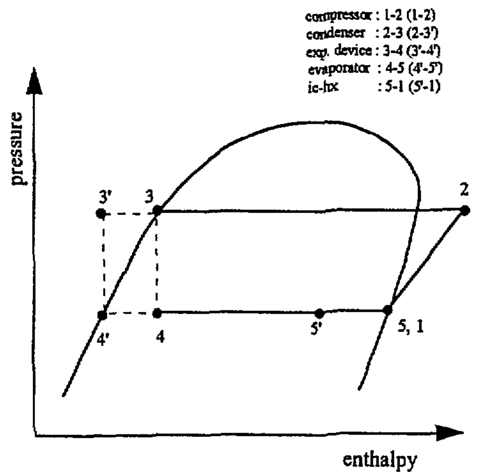

(a)

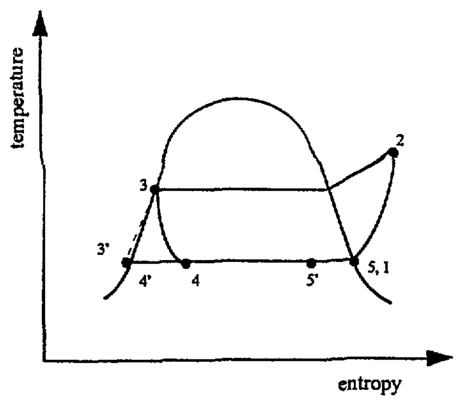

(b)

Figure 2. Basic vapor compression cycle and the cycle with intracycle evaporative cooling

Table 1. Seleted Properties of Tested Refrigerants at Atmospheric Pressure

Refrigerant	Molecular Weight (g/mol)	Bubble-Point/ Dew-Point (℃)	Temperature Glide (℃)	Liquid Conductivity (W/m℃)	Liquid Viscosity (μP)
R22	86.47	-40.8/-40.8	0.0	0.1286	336.9
R407C (23/25/52)	86.20	-43.8/-36.7	7.1	0.1380	428.0
R32/152a (50/50)	58.34	-43.7/-35.6	8.1	0.1804	308.5
R23/152a (20/80)	66.81	-51.7/-28.6	23.1	0.1590	368.9

Note: Mass composition is used to define mixtures.

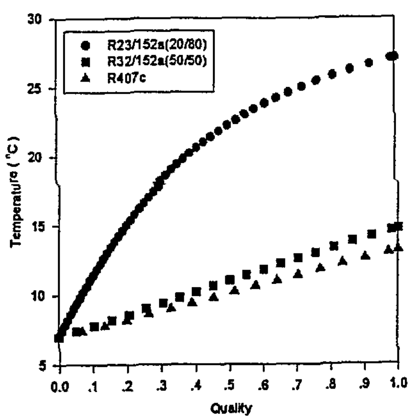

Figure 3. Temperature glides at pressures corresponding to 7 ℃ bubble-point temperature

The following list shows the input data for the simulations:

- temperature of HTF entering/leaving the evaporator, 13 ℃/7 ℃
- temperature of HTF entering/leaving the condenser, 29 ℃/35 ℃
- superheat at the compressor inlet, 0.0 ℃
- polytropic compression effciency, 0.85
- subcooling at the condenser outlet, 0.0 ℃
- pressure drop in the condenser, 0.0
- pressure drop in the evaporator, 0.0
- pressure drop in the ic-hx, 0.0

Simulations were performed for several different vapor qualities leaving the evaporator and entering the ic-hx. Because saturated vapor was imposed at the compressor inlet for all simulations, different vapor qualities leaving the evaporator corresponded to different heat transferred between the low-pressure two-phase refrigerant and the high-pressure subcooled liquid. Additional simulations were conducted for a basic system (not involving the ic-hx) to obtain a performance reference point.

Figure 4 presents the simulation results graphical form. The figure shows the coefficient of performance (COP) and compressor power referenced to those of the basic cycle. Implementation of the ic-hx did not change performance of R-22, but it improved the performance of the mixtures. The maximum COP of mixtures occurs at the highest amount of heat transferred in the ic-hx, which corresponds to the lowest quality of refrigerant leaving the evaporator. For this condition, the COP improvement is similar for all three mixtures (approximately 3%). The compressor power changed insignificantly with the use of ic-hx. This implies that the COP improvement displayed in Figure 4 was caused by an increase in capacity.

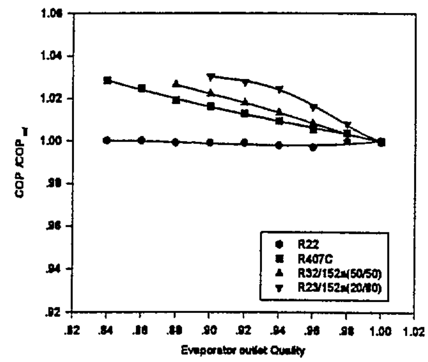

(a)

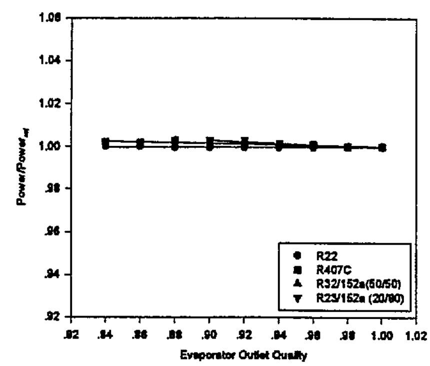

(b)

Figure 4. Simulated COP and compressor power referenced to the basic vapor compression cycle

It should be noted that R-32/152a and R407C have a linear temperature glide similar in magnitude to that of the heat-transfer fluids. On the other hand, the glide of R-23/152a is nearly twice of this magnitude and highly nonlinear in the low quality region (Figure 3), which results in a glide mismatch. The similar COP improvement potential for these three mixtures indicates the importance of glide matching between refrigerant and heat-transfer fluid, and it discounts the significance of a high glide as a stand-alone merit.

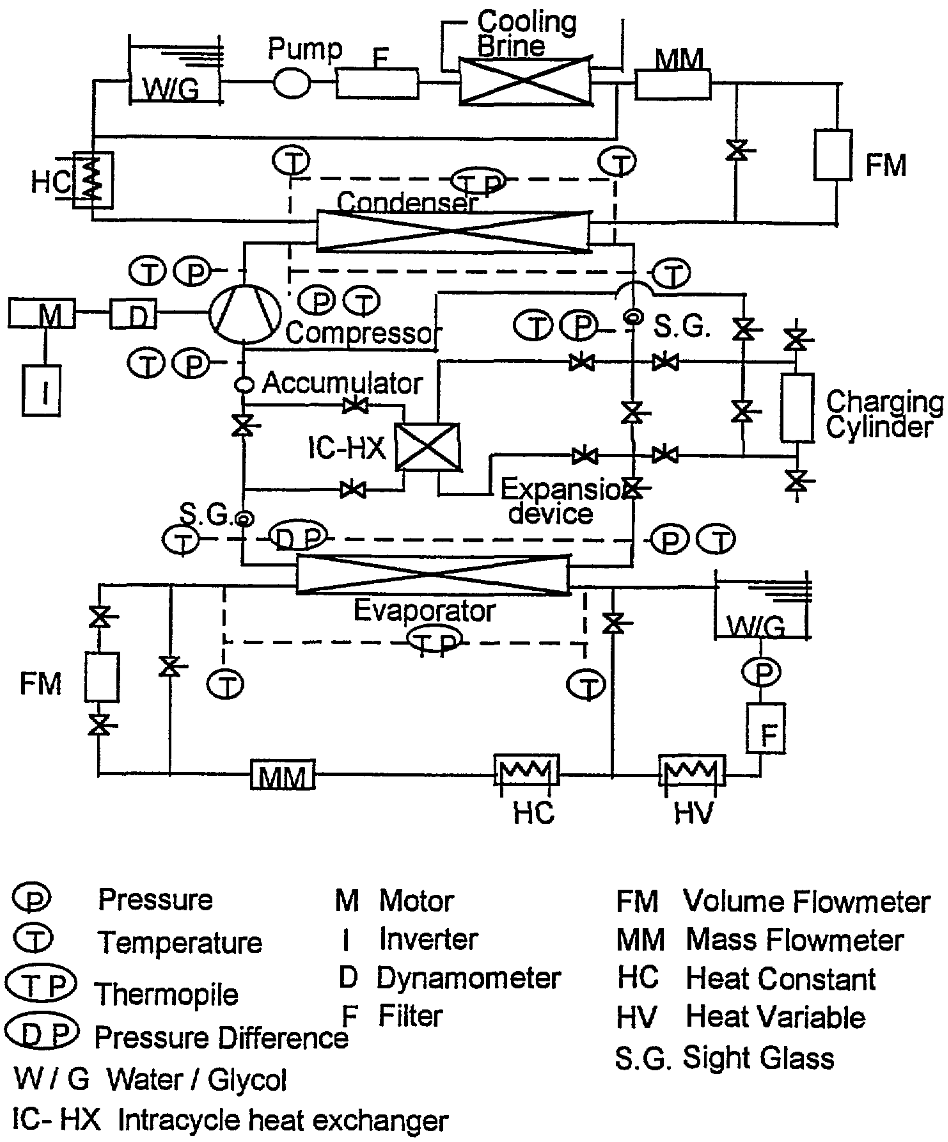

Fig 5. Schematic of the Small Breadboard Heat Pump

LABORATORY EXPERIMENT

Test Facility The study was performed using an experimental apparatus referred to as a Small Breadboard Heat Pump(SBHP). This apparatus has been used in a few previous NIST projects, starting with the investigation by Pannock and Didion.[8] A few modifications were made to the original apparatus to facilitate the studying the ic-hx cycle. Figure 5 shows a schematic of the modified system.

The refrigerant side of the SBHP consisted of the compressor, condenser, intracycle heat exchanger, expansion device, and evaporator. The system employed an open, two-cylinder reciprocating compressor of 45 cm^3 total displacement. The inverter maintained compressor speed constant at 800 RPM during all tests. Commercially available torque and RPM transducers were used to measure the revolution speed and torque. The mineral oil that was originally supplied with the compressor was used with all four refrigerants tested.

The condenser and evaporator had a counterflow tube-in-tube configuration and used a water/ethylen-glycol (40/60) mixture as the heat transfer fluid. After leaving the condenser, the refrigerant flowed either directly to the expansion device, or first to the ic-hx and then to the expansion device. From the evaporator, the refrigerant flowed to the compressor either directly or through the low-pressure side of the ic-hx. The ic-hx assembly comprised four identical heat exchangers, which could be brought on line independently to vary the heat-transfer area.

Refrigerant temperature and pressure were measured by thermocouples and pressure transducers placed in key locations of the refrigerant loop. Additionally, thermocouples were installed throughout the heat exchanger to measure the temperature profiles of the refrigerant and HTF. The thermocouples were type T and were surface-mounted. Temperature change of the HTF across the heat exchangers was measured by ten-junction thermopiles located at the inlet and outlet of the condenser and evaporator. A data acquisition/countrol unit connected to a personal computer used to control system operation and test conditions as well as for collection of test data.

Test Procedure The tests were conducted at the same HTF temperatures as those used in the CYCLE-11 simulations. The inlet temperatures were controlled by electric heaters, and the outlet temperatures were controlled by adjusting HTF mass flow rates. Refrigerant subcooling at the condenser outlet was maintained at 4 ± 2 ℃ for all tests. On the low-pressure side, the refrigerant superheat at the compressor inlet was maintained at 5 ± 2 ℃. For the system with the ic-hx, the refrigerant leaving the evaporator was two-phase, which was confirmed by a combination of visual observation through the sight glass and measurement of the refrigerant temperature profile in the evaporator. The refrigerant charge and expansion valve opening were adjusted to obtain the specified superheat and subcooling for a given combination of intracycle heat maintained within ± 0.1 ℃ of the temperature set points for at least 15 minutes.

The experimental rig was charged by weight from containers holding individual refrigerants. A gas chromatograph was used for determining composition of the mixtures. The analysis was performed using a small amount of vapor taken from the compressor discharge line after the system reached steady-state operation. The circulating mass compositions were 24/27/59 for R32/125/134a, 47/53 for R32/152a, and 23/77 for R23/152a. The deviation of these compositions from those employed in simulations were not large enough to make appreciable impact on performance (this was verified with additional CYCLE-11 simulations). Therefore, for simplicity of presentation, the rounded compositions from simulation runs are uniformly used to identify the fluids studied.

Test Results The test results for COP and capacity are presented graphically in Figures 7 and 8. In these figures, the horizontal dotted line denotes the reference performance of a system without the ic-hx for the same refrigerant. Among the four fluids tested, the R32/152a mixture had the highest reference COP (5.15), followed by that of R22(4.94), R407C (4.67), and R23/152a(4.41). The R23/152a mixture displayed a low COP despite a significantly lower capacity than other fluids. The highest reference capacity was measured for R407C. Reference capacities of R22 and R32/152a were within 3.3% of that of exchangers. System operating parameters were recorded after the HTF temperatures were R407C, and reference capacity for R23/152a was 23% lower. All three mixtures benefited from the ic-hx, while the COP of R22 deteriorated, as shown in Figure 6. The COP increases for mixtures were 4.0% for R32/152a, 3.6% for R407C, and 1.8% for R23/152a. These COP increases were calculated using the averages of COPs for the tests with 88-90% refrigerant quality at the evaporator exit. The data points for 100% evaporator outlet quality represent the results from a few tests with different superheats at the evaporator exit. Because of the superheat, the system capacities were lower, which resulted in the low COPs shown in Figure 6. Also, more superheated (higher temperature) vapor required more specific vapor required more specific compression work because of a lower density. This was additional negative effect on the system COP, although not as significant as that due to decrease in evaporator capacity.

Figure 7 shows the measured capacities. The use of the ic-hx did not affect the capacity of R22., but increased capacities of the mixtures. Compared with the reference value from the tests without the ic-hx, the maximum capacity improvement was approximately 7.0% for R32/152a (50/50), 3.4% for R407C, and 4.4% for R23/152a (20/80). The use of the ic-hx did not affect significantly the pressure in the condenser. However, the suction pressure increased with the amount of heat transferred in the ic-hx.

Figure 8 shows the compressor suction

pressure for R23/152a. The pressure trend shown in this figure is typical for other mixtures. An increase of the suction pressure reduces the specific work needed to compress the refrigerant to the condenser pressure, improving system efficiency. As expected, no change of suction (evaporator) pressure was measured for R22.

Figure 9, 10 and 11 present HTF and refrigerant temperature profiles in the evaporator. Refrigerant temperatures were measured by thermocouples surface-mounted on the return bends of the heat exchangers. Because of the bend design and space limitation, some heat conduction took place between the refrigerant and HTF at the measurement locations. This heat transfer manifests itself by a seesaw profile which is particularly visible for the HTF. Even with this shortcoming, the temperature profiles shown for the evaporator and condenser can be used in comparative, qualitative analysis.

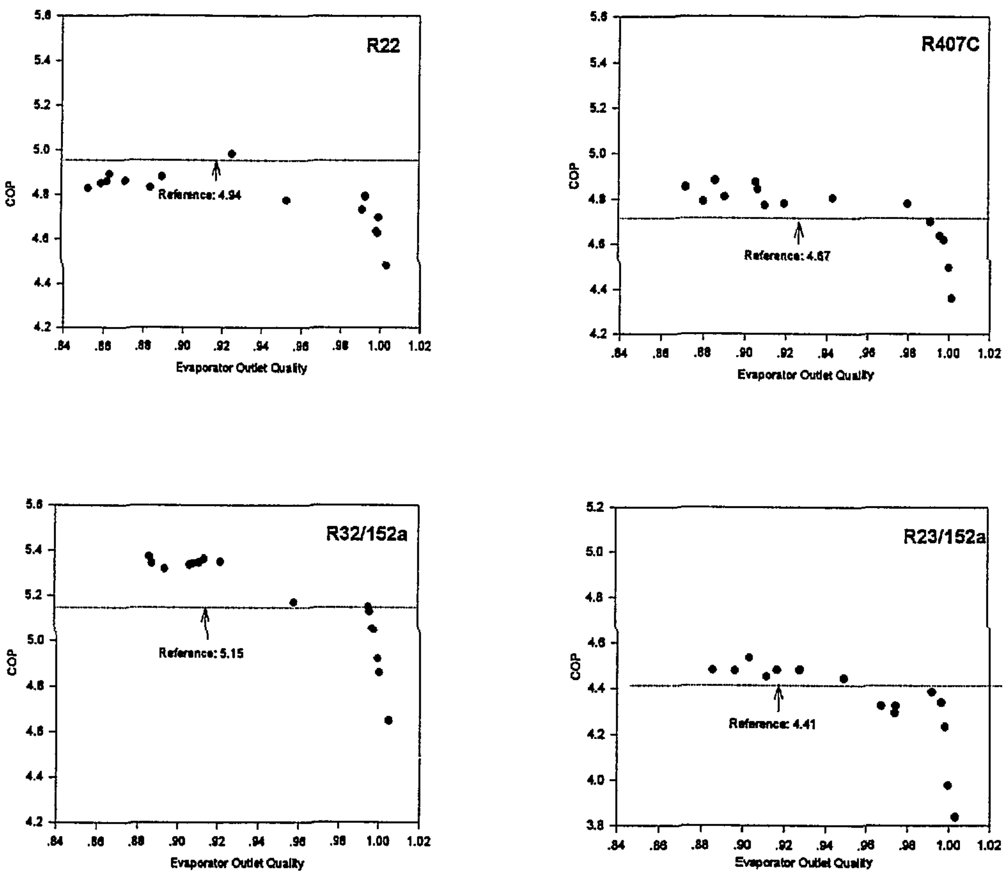

Figure 6. Measured COP of R22, R407C, R32/152a(50/50), and R23/152a(20/80)

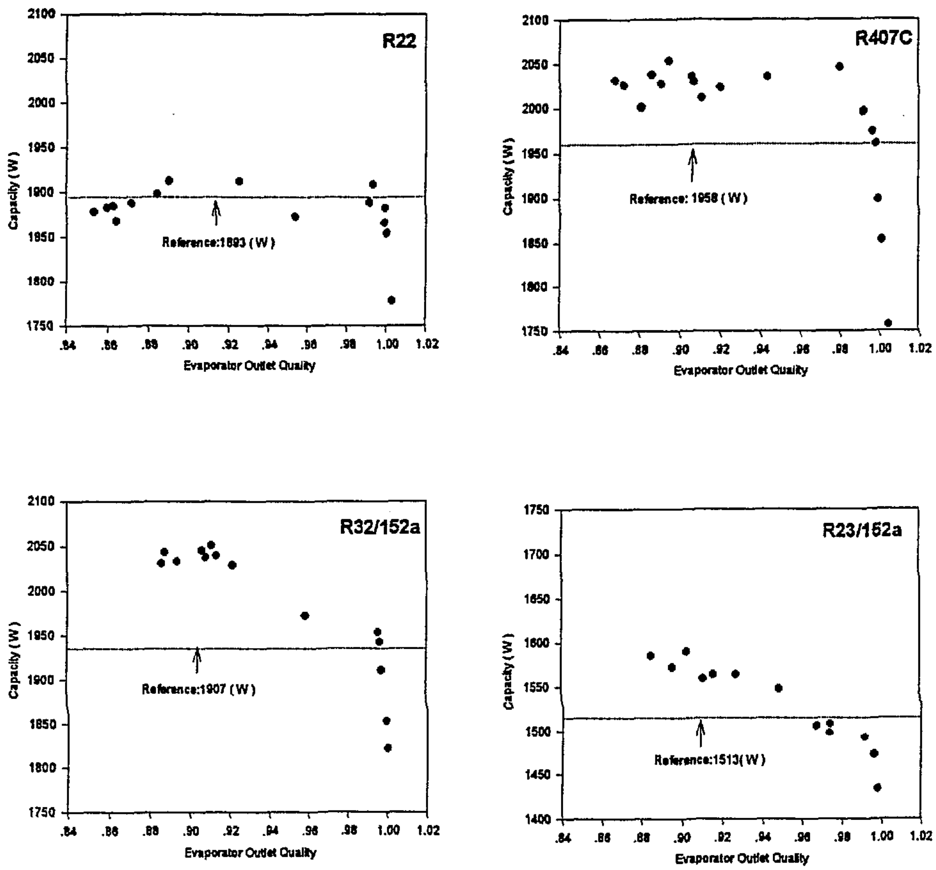

Figure 7. Measured capacity of R22, R407C,R32/152a(50/50), and R23/152a(20/80)

Figures 9 and 10 show the temperature profiles for the basic system and ic-hx system working with R407C. The refrigerant profile for the ic-hx system does not have a superheated vapor spike because vapor superheating takes place in the ic-hx. The temperature of the evaporating refrigerant is higher in the ic-hx system than in the basic system.

The poor performance of R23/152a, both in the basic and modified cycle, can be explained by the mismatched temperature profiles in the evaporator and condenser. Figure 11 shows that R23/152a displays significant nonlinearity in the low-quality region in the evaporator. A similar nonlinear temperature profile was also present in the condenser where a strong pinch point occurred. R23/152a achieved the lowest

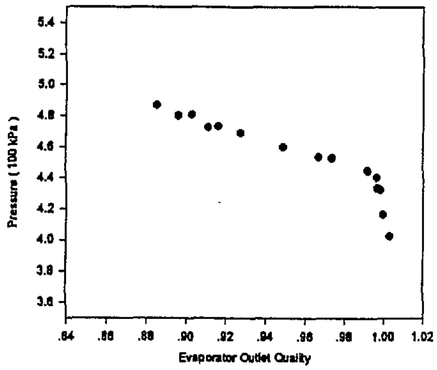

Figure 8. Compressor suction pressure for R23/152a(20/80)

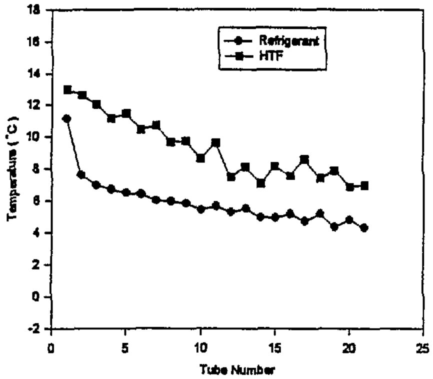

Figure 9. Temperature profiles of evaporator with R407C in the system without ic-hx

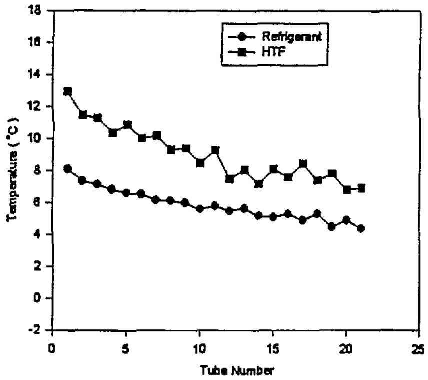

Figure 10. Temperature profiles of evaporator with R407C in the system with ic-hx

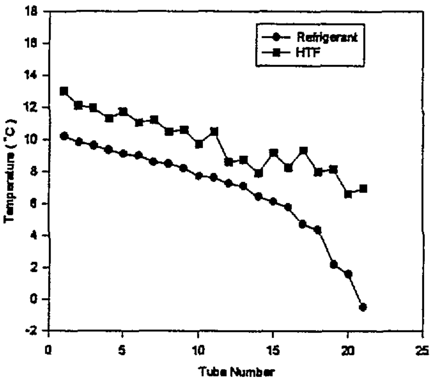

Figure 11. Temperature profiles of evaporator with R23/152a(20/80) in the system with ic-hx

COP among the tested fluids in spite of the lowest capacity. Typically, a low-capacity refrigerant has a better COP than the higher-capacity fluid when evaluated in a given system[9]. The preceding observations allow us to make a general comment regarding high-glide zeotropic mixtures. It appears that high-glide binary mixtures, like R23/152a having over 20 ℃ glide, will inherently have a very nonlinear temperature profile (Figure 3). Such mixtures will perform poorly in heat exchangers because common heat-transfer fluids have a nearly constant heat capacity and linear temperature profile. The mismatch in temperature profiles will result in significant heat-transfer irreversibilities, which will cause the poor system performance.

CONCULDING REMARKS

Evaporative cooling of the refrigerant leaving the condenser by a two-phase refrigerant leaving the evaporator improves the performance of zeotropic mixtures. The laboratory tests showed that the COP of the zeotropic mixtures improved with evaporative cooling while the performance of R22 did not. The COP increase was 4.0% for R32/152a (50/50), 3.6% for R407C, and 1.8% for R23/152a (20/80). The cooling capacity increased by 7.0% for R32/152a, 3.4% for R407C, and 4.4% for R23/152a. It can be inferred that intracycle evaporative cooling was not the only reason for the improved performance of the ic-hx system; most likely the elimination of superheated refrigerant at the evaporator exit and a corresponding change in the refrigerant-side heat-transfer coefficient also contributed to the performance change. On an absolute scale, R32/152a (50/50) showed the best COP, followed by R22,R407C, and R23/152a(20/80). The simulation results showed the performance trends consistent with those measured in the laboratory.

ACKNOWLEDGEMENTS

This study was sponsored by the U.S. Department of Energy, Office Building Technology. Mr. William Noel served as the project manager. The authors would like to thank Mr. Pete Rothfleisch and Mr. John Wamsley of NIST for their assistance. Financial support by LG Electronics, Inc. for Mr. Kim during his stay at NIST is also acknowledged.

REFERENCES

1. Domanski, P.A., "Minimizing Throttling Losses in the Refrigerant Cycle", Proceedings of the int. Congr. Refrig., The Hague, The Netherlands, Vol. 4b, 1995.
2. Vakil, H.B., "Thermodynamics of heat exchange in refrigeration cycles with non-azeotropic mixtures. Part II, Suction heat exchange and evaporative cooling of capillary", Proceeding XVI Int. Congr. Refrig., Paris, France, IIR, Commission B1, 1983.
3. Mulroy, W., Kauffeld, M., McLinden, M., and Didion, D., "An Evaluation of Two Refrigerant Mixtures in a Breadboard Air Conditioner", Proceedings of the IIR-Purdue Conference, IIR, Paris, France, 1988.
4. Domanski, P.A., Didion, D.A., Mulroy, W.J., and Parise, J., "A Simulation Model and Study of Hydrocarbons Refrigerants for Residential Heat Pump Systems", Proceedings of the Intenational Conference on New Applications of Natural Fluids in Refrigeration and Air Conditioning, Hanover, Germany. IIR, Paris,

France, 1994.

5. Choi, D.K., Domanski, P.A., and Didion, D.A., "Laboratory Evaluation of Flammable Refrigerants for Application in a water-to-Water Heat Pump", NISTIR(to be published), National Institute of Standards and Technology, Gaithersburg, MD, 1995.

6. Gallager, J.,McLinden,M.O., Morison,O. and Huber,M., "NIST Standard Reference Data Base 23, Version 4.01"(REFPROP), National Institute of Standards and Technology, Gaithersburg, MD, USA, 1993.